

# Effect of pulse current on structure and adhesion of apatite electrochemically deposited onto titanium substrates

Tomoyasu Hayakawa

*Photonics and Electronics Science and Engineering Center, Graduate School of Engineering, Kyoto University, Nishikyo-ku, Kyoto 615-8510, Japan*

Masakazu Kawashita<sup>a)</sup>

*Center for Research Strategy and Support, Tohoku University, Aoba-ku, Sendai 980-8579, Japan*

Gikan H. Takaoka

*Photonics and Electronics Science and Engineering Center, Graduate School of Engineering, Kyoto University, Nishikyo-ku, Kyoto 615-8510, Japan*

Toshiki Miyazaki

*Graduate School of Life Science and Systems Engineering, Kyushu Institute of Technology, Wakamatsu-ku, Kitakyushu 808-0196, Japan*

(Received 20 April 2008; accepted 15 August 2008)

Apatite films were deposited onto titanium (Ti) metal substrates by an electrodeposition method under a pulse current. Metastable calcium phosphate solution was used as the electrolyte. The ion concentration of the solution was 1.5 times that of human body fluid, but the solution did not contain magnesium ions at 36.5 °C. We used an average current density of 0.01 A/cm<sup>2</sup> and current-on time ( $T_{\text{ON}}$ ) equal to current-off time ( $T_{\text{OFF}}$ ) of 10 ms, 100 ms, 1 s, and 15 s. The adhesive strength between apatite and Ti substrates were relatively high at  $T_{\text{ON}} = T_{\text{OFF}} = 10$  ms. It is considered that small calcium phosphate (C–P) crystals with low crystallinity were deposited on the Ti surface without reacting with other C–P crystals, H<sub>2</sub>O, and HCO<sub>3</sub><sup>−</sup> in the surrounding environment. This resulted in relaxation of the lattice mismatch and enhancement of the adhesive strength between the apatite crystals and Ti substrates.

## I. INTRODUCTION

Titanium (Ti) metal and its alloys are widely used for orthopedic and dental applications because they exhibit high mechanical properties and biocompatibility.<sup>1–3</sup> Ti metal has a passive layer of TiO<sub>2</sub> on its surface, which is responsible for its chemical stability and therefore its biocompatible characteristics. This oxide layer naturally has a thickness of a few nanometers, but the thickness can be increased to a few micrometers by chemical and thermal treatments.<sup>4</sup> Although Ti metal is biocompatible, it is not bioactive and hence it cannot directly bond to living bones. To improve its bone-bonding property, apatite coating is applied on Ti implants.<sup>5</sup> Several coating methods, such as plasma spraying,<sup>6</sup> biomimetic precipitation,<sup>7,8</sup> and electrodeposition,<sup>9–11</sup> have been successfully used to deposit an apatite layer on Ti or titanium alloy implants. Each of these methods has some advantages as well as drawbacks. Among these coating tech-

niques, only the plasma spraying of apatite is clinically used. However, the high temperature of the plasma flame may adversely affect the implant structure and the homogeneity of the coating, resulting in delamination of the coating.<sup>12–14</sup>

The electrodeposition method is an alternative process that uses aqueous solutions at low temperatures; this method hardly affects the implant structure and can be applied to complex shapes.<sup>15</sup> In addition, the apatite layer can be rapidly formed on Ti substrates by electrodeposition in a metastable calcium phosphate solution whose ion concentration is 1.5 times that of a normal simulated body fluid (SBF), and does not contain MgCl<sub>2</sub>·6H<sub>2</sub>O.<sup>16</sup> However, this method increases the pH at the interface between Ti and the electrolyte due to electron incorporation to form OH<sup>−</sup> ions and H<sub>2</sub> through water reduction.<sup>17</sup> The H<sub>2</sub> gas evolution at the interface leads to a heterogeneous coating.<sup>15</sup> Furthermore, the adhesive strength between apatite and the substrate is often low and the total amount of apatite crystals deposited on the Ti substrate is much smaller than that theoretically calculated from the total electric charge.<sup>18</sup> To solve this problem, new approaches are needed in the electrodeposition

<sup>a)</sup>Address all correspondence to this author.

e-mail: m-kawa@ecei.tohoku.ac.jp

DOI: 10.1557/JMR.2008.0386

method. Our previous studies revealed that electrodeposition under a long pulse ( $>5$  s) was more effective for crystal growth and apatite formation than that under direct current.<sup>19</sup> The studies also revealed that when the Ti metals were previously etched in 50% or 75% sulfuric acid ( $\text{H}_2\text{SO}_4$ ) followed by electrodeposition and then heat treatment, a dense and uniform apatite layer with good adhesive properties was formed onto the Ti substrates.<sup>20</sup> However, pyrophosphate ( $\text{P}_2\text{O}_7^{4-}$ ) compound, an inhibitor of mineralization,<sup>21</sup> was formed in apatite crystals during heat treatment.

The purpose of the present work is to coat an apatite layer on Ti substrates with good adhesion in metastable calcium phosphate solution by using various pulse widths without subsequent heat treatment and to investigate the effect of pulse width on the apatite coatings and adhesive strength.

## II. EXPERIMENTAL

Rectangular specimens of Ti substrates (purity: 99.5%, The Nilaco Corporation, Tokyo, Japan) with a volume of  $10 \times 10 \times 1 \text{ mm}^3$  were abraded with a #400 diamond plate and then washed with acetone, ethanol, and ultrapure water in an ultrasonic cleaner.

Before the electrodeposition under pulse current (PE), the Ti substrates were etched in  $30 \text{ cm}^3$  of  $\text{H}_2\text{SO}_4$  with a concentration of 75%, which was prepared by diluting 97%  $\text{H}_2\text{SO}_4$  (Nacalai Tesque Inc., Kyoto, Japan) with ultrapure water at  $60^\circ\text{C}$  for 30 min. After etching, the specimens were washed with ultrapure water.

PE was performed in a two-electrode cell configuration. The Ti specimens were used as the cathode, and a platinum plate (HX-C2, Hokuto Denko Corp., Tokyo, Japan) was used as the counter electrode. At a current-on time ( $T_{\text{ON}}$ ) of 15 s, the pulse current was applied by a function generator (Agilent 33120A, Agilent Technologies Inc., Tokyo, Japan). At a  $T_{\text{ON}}$  of 10 ms, 100 ms, and 1 s, the pulse current was applied by a controlled current pulse generator (HC-110, Hokuto Denko Corp., Tokyo, Japan). The average current density was  $0.01 \text{ A/cm}^2$ , and  $T_{\text{ON}}$  was equal to the current-off time ( $T_{\text{OFF}}$ ) irrespective of the pulse width. The electrolyte was  $60 \text{ cm}^3$  of 1.5SBF (simulated body fluid) without magnesium  $\text{Mg}^{2+}$  ions at  $36.5^\circ\text{C}$ . In this study, to enhance the growth of apatite, the ion concentration of the solution was increased up to 1.5 times that of normal SBF,<sup>22</sup> but  $\text{Mg}^{2+}$  ions, an inhibitor of hydroxyapatite precipitation and growth,<sup>23</sup> were eliminated in the electrolyte. Table I shows the amounts of reagents for the preparation of 1.5SBF without  $\text{Mg}^{2+}$  ions. This electrolyte was prepared by dissolving reagent grade chemicals of NaCl,  $\text{NaHCO}_3$ , KCl,  $\text{K}_2\text{HPO}_4 \cdot 3\text{H}_2\text{O}$ ,  $\text{CaCl}_2$ , and  $\text{Na}_2\text{SO}_4$  (Nacalai Tesque Inc., Kyoto, Japan) in ultrapure water. The pH of the electrolyte was adjusted to 7.40 with tris(hydroxy-

TABLE I. Amounts of reagents for preparation of 1.5SBF without  $\text{Mg}^{2+}$  ions.

	Reagent	Amount/g	Purity/%
1	NaCl	11.994	99.5
2	$\text{NaHCO}_3$	0.525	99.5
3	KCl	0.336	99.5
4	$\text{K}_2\text{HPO}_4 \cdot 3\text{H}_2\text{O}$	0.342	99.0
5	1.0M-HCl	$48 \text{ cm}^3$	...
6	$\text{CaCl}_2$	0.417	95.0
7	$\text{Na}_2\text{SO}_4$	0.107	99.0
8	$(\text{CH}_2\text{OH})_3\text{CNH}_2$	9.086	99.0
9	1.0M-HCl	$\sim 15 \text{ cm}^3$	...

methyl)aminomethane [ $(\text{CH}_2\text{OH})_3\text{CNH}_2$ ] and  $1.0 \text{ mol/dm}^3$ -HCl aqueous solution (Nacalai Tesque Inc., Kyoto, Japan) at  $36.5^\circ\text{C}$ . The deposition times were 90 min, because our previous study<sup>16</sup> demonstrated that uniform apatite deposition was achieved by electrodeposition over 90 min. After the electrodeposition, the specimens were gently washed with ultrapure water and then dried at  $40^\circ\text{C}$  for 24 h.

The surface structure of the specimens was investigated by field-emission scanning electron microscopy (FE-SEM; S-4500, Hitachi Ltd., Tokyo, Japan), thin-film x-ray diffraction (TF-XRD; Rigaku RINT-2500, Tokyo, Japan), and Fourier transform infrared reflection spectroscopy (FTIR; Nicolet Magna 860, Thermo Electron K.K., Kanagawa, Japan). The thickness of the products deposited on the Ti substrates by PE was measured by FE-SEM. The surface roughness (arithmetic average roughness:  $R_a$ ) of the substrates was measured by atomic force microscopy (AFM; SPA300, Seiko Instruments Inc., Tokyo, Japan).

The adhesion between apatite and the substrates was evaluated by a peeling test using Scotch tape (810, Sumitomo 3M Ltd., Tokyo, Japan) and by a scratch test using a surface property tester (Type 14DR, Shinto Scientific Corp. Ltd., Tokyo, Japan) equipped with a sapphire needle (diameter of  $50 \mu\text{m}$ ). In the scratch test, constant loads of 50, 100, and 200 g were applied to the scratch needle.

## III. RESULTS AND DISCUSSION

Figures 1 and 2 show the FE-SEM photographs and the TF-XRD patterns of the surface of both the unetched Ti substrates and those etched in 75%  $\text{H}_2\text{SO}_4$ , respectively. We confirmed that microstructural roughness was formed by the acid etching. The  $R_a$  of the unetched substrate was  $0.116 \mu\text{m}$ , while that of the etched substrate was  $0.186 \mu\text{m}$ . The reactions taking place during the etching of the Ti substrate in 75%  $\text{H}_2\text{SO}_4$  are shown below.<sup>24</sup>

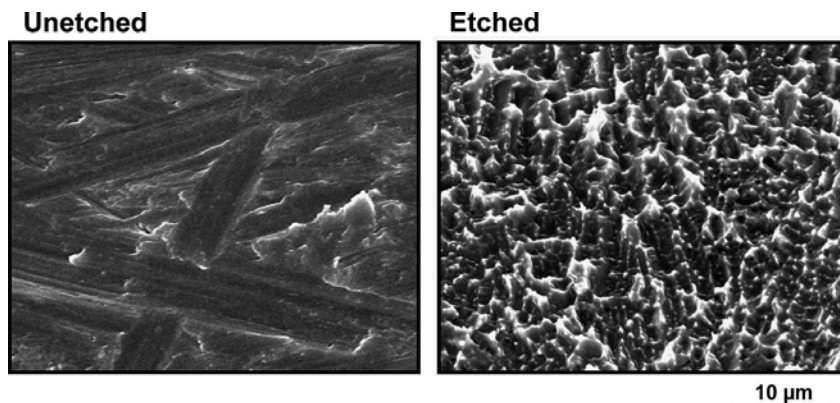


FIG. 1. FE-SEM photographs of surfaces of Ti substrates unetched and etched in 75% H<sub>2</sub>SO<sub>4</sub>.

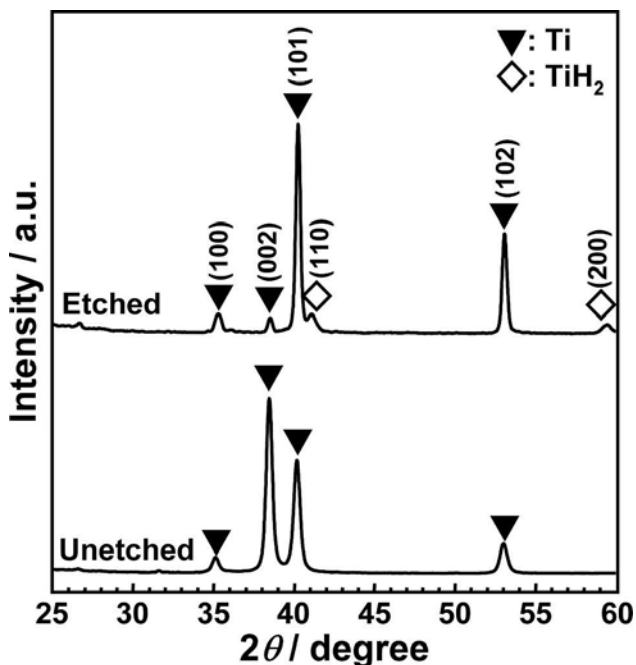
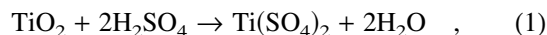


FIG. 2. TF-XRD patterns of surfaces of Ti substrates unetched and etched in 75% H<sub>2</sub>SO<sub>4</sub>.



According to the above chemical reaction (3), TiH<sub>2</sub> will be formed on the Ti substrates by the acid treatment. Indeed, we can confirm XRD peaks of TiH<sub>2</sub> around 40.9° and 59.6° in 2θ, as shown in Fig. 2 and our previous study.<sup>20</sup>

Figure 3 shows the TF-XRD patterns of the unetched and etched Ti substrates subjected to PE at various  $T_{\text{ON}}$ . For all specimens, the peaks assigned to apatite were observed at around 26°, 28°, and 32° in 2θ.<sup>25</sup> Furthermore, the diffraction peak due to (202) of apatite was observed at around 36° in 2θ for the specimens at  $T_{\text{ON}} = 15$  s. The existence of the diffraction peaks of apatite means that apatite was successfully deposited on the Ti metal surface by PE. The diffraction peaks of apatite for the specimens at  $T_{\text{ON}}$  above 1 s were stronger than those at  $T_{\text{ON}}$  below 100 ms. Figure 4 shows the total intensities of the diffraction peaks of apatite at various  $T_{\text{ON}}$ . The intensity of apatite tended to decrease with decreasing

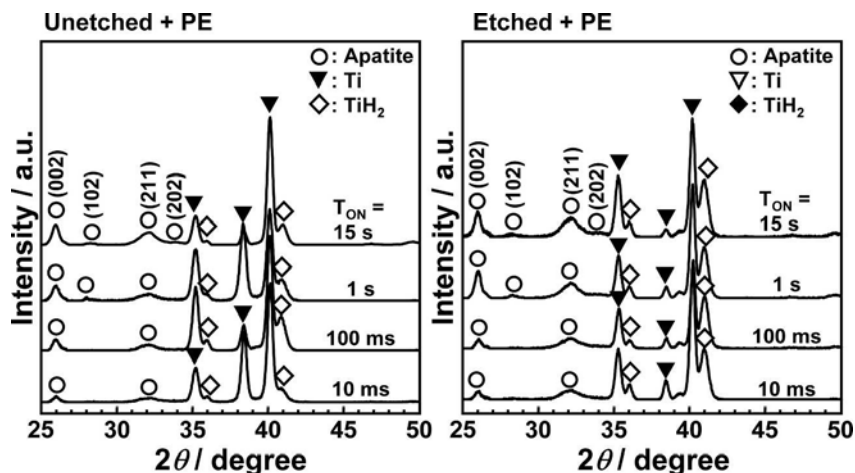


FIG. 3. TF-XRD patterns of surfaces of unetched and etched Ti substrates subjected to electrodeposition at various  $T_{\text{ON}}$ .

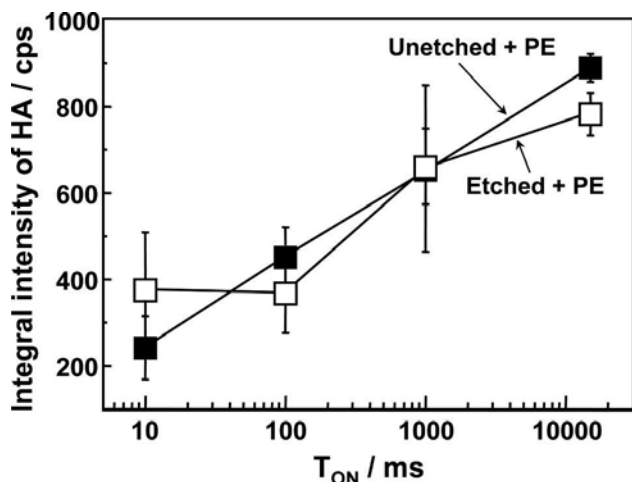


FIG. 4. Thickness of products deposited on Ti substrates as a function of  $T_{ON}$ .

$T_{ON}$ . The decrease in intensity indicates a decrease in the weight fraction of apatite in the crystals on the surface comprising Ti metal, apatite crystals, and calcium phosphate [ $\text{Ca}_3(\text{PO}_4)_2$ , C-P] crystals.<sup>26</sup> Figure 5 shows the thickness of the products, comprising apatite and/or C-P,<sup>17</sup> formed on Ti substrates by PE at various  $T_{ON}$ . The figure shows that there is no correlation between the thickness of the products deposited on the Ti substrates and  $T_{ON}$ . Therefore, it is considered that the pulse width affects the weight fraction of apatite in the products deposited on the Ti substrates, but not the total amount of products deposited by PE. According to Figs. 3 and 4, it is considered that the weight fraction of apatite crystals in the products deposited on the Ti substrates kept decreasing with  $T_{ON}$ . This indicates that the crystal growth of apatite was suppressed with a decrease in  $T_{ON}$ .

Figure 6 shows the FTIR spectra of the unetched and etched Ti substrates, which were subjected to PE at vari-

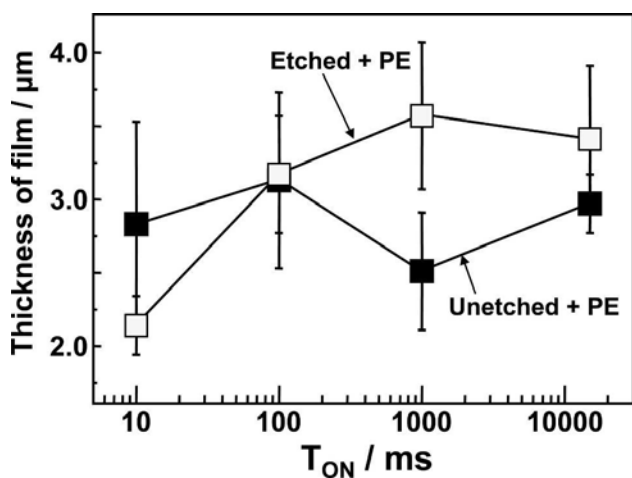


FIG. 5. Total intensities of diffraction peaks of apatite as a function of  $T_{ON}$ .

ous  $T_{ON}$ . In Fig. 5, all spectra showed  $\text{PO}_4^{3-}$  absorption bands<sup>27</sup> at 1100–1000, 960, 600, and 580  $\text{cm}^{-1}$ , an  $\text{OH}^-$  band at 1650  $\text{cm}^{-1}$ , and a  $\text{CO}_3^{2-}$  band<sup>28</sup> or  $\text{HPO}_4^{2-}$  band<sup>29</sup> at 865  $\text{cm}^{-1}$ . Furthermore, the spectra of the unetched Ti substrates subjected to PE at  $T_{ON}$  above 100 ms and those of the etched Ti substrates subjected to PE at  $T_{ON}$  above 1 s showed  $\text{CO}_3^{2-}$  bands at 1540–1350  $\text{cm}^{-1}$ . The existence of this band indicates that carbonate-containing apatite crystals and/or  $\text{CaCO}_3$  were deposited onto the substrate by PE.<sup>18</sup> The intensity of  $\text{CO}_3^{2-}$  adsorption bands at 1540–1350  $\text{cm}^{-1}$ ,  $\text{PO}_4^{3-}$  absorption band at 960  $\text{cm}^{-1}$ , and  $\text{CO}_3^{2-}$  band<sup>28</sup> or  $\text{HPO}_4^{2-}$  band at 865  $\text{cm}^{-1}$  decreased with  $T_{ON}$ . This indicates that the amount of  $\text{CO}_3^{2-}$  in apatite and/or  $\text{CaCO}_3$  and the fraction of apatite crystals in the deposited products on the Ti substrates decrease with  $T_{ON}$ . However, it is considered that the acid etching hardly affects the crystal structure of apatite because similar TF-XRD patterns and FTIR spectra were obtained for both the unetched and etched Ti substrates.

Figure 7 shows the FE-SEM photographs of the unetched and etched Ti substrates subjected to PE at various  $T_{ON}$ . For each specimen, the left side is the FE-SEM photograph of the unetched Ti substrates subjected to PE at various  $T_{ON}$ , and the right side is that of the etched Ti substrates subjected to PE at various  $T_{ON}$ . These photographs show that dense uniform layers were formed on the surfaces of all specimens. Figures 3 and 6 show these layers might be apatite. It was found that the apatite crystals on all specimens had cracks. These cracks might be formed by vaporization of moisture in apatite crystals, when the substrates were dried in air at room temperature after the electrodeposition. The width of the cracks decreased with  $T_{ON}$ . During plating, it is known that amorphous thin films have no cracks on its surface.<sup>30</sup> Similarly in this study, it is considered that the increase in the amorphous component of the products decreased the crack width.

Figure 8 shows the FE-SEM photographs of the unetched and etched Ti substrates subjected to PE at various  $T_{ON}$  followed by the peeling test using Scotch tape. The deposited apatite was easily peeled off by the Scotch tape for the etched and unetched Ti substrates subjected to PE at  $T_{ON} = 1$  s and 15 s (see Fig. 7). However, it did not peel off (with the glue of the Scotch tape remaining on the surface) from the etched Ti substrates subjected to PE at  $T_{ON} = 10$  ms and 100 ms and the unetched Ti substrates subjected to PE at  $T_{ON} = 10$  ms. The glue of the Scotch tape that remained on the surface indicates that the adhesive strength of the apatite coating of these specimens was relatively high. The cracks did not extend outside the scratch trace, and the apatite films deposited on the etched Ti substrates subjected to PE at  $T_{ON} = 10$  ms and 100 ms did not come off even though a high load of 200 g was applied to the scratch needle. The results for

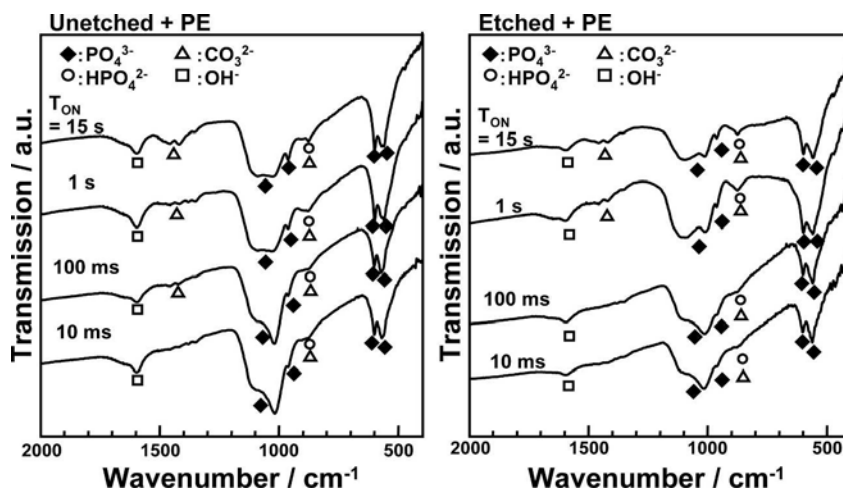


FIG. 6. FTIR spectra of unetched and etched Ti substrates subjected to electrodeposition at various  $T_{ON}$ .

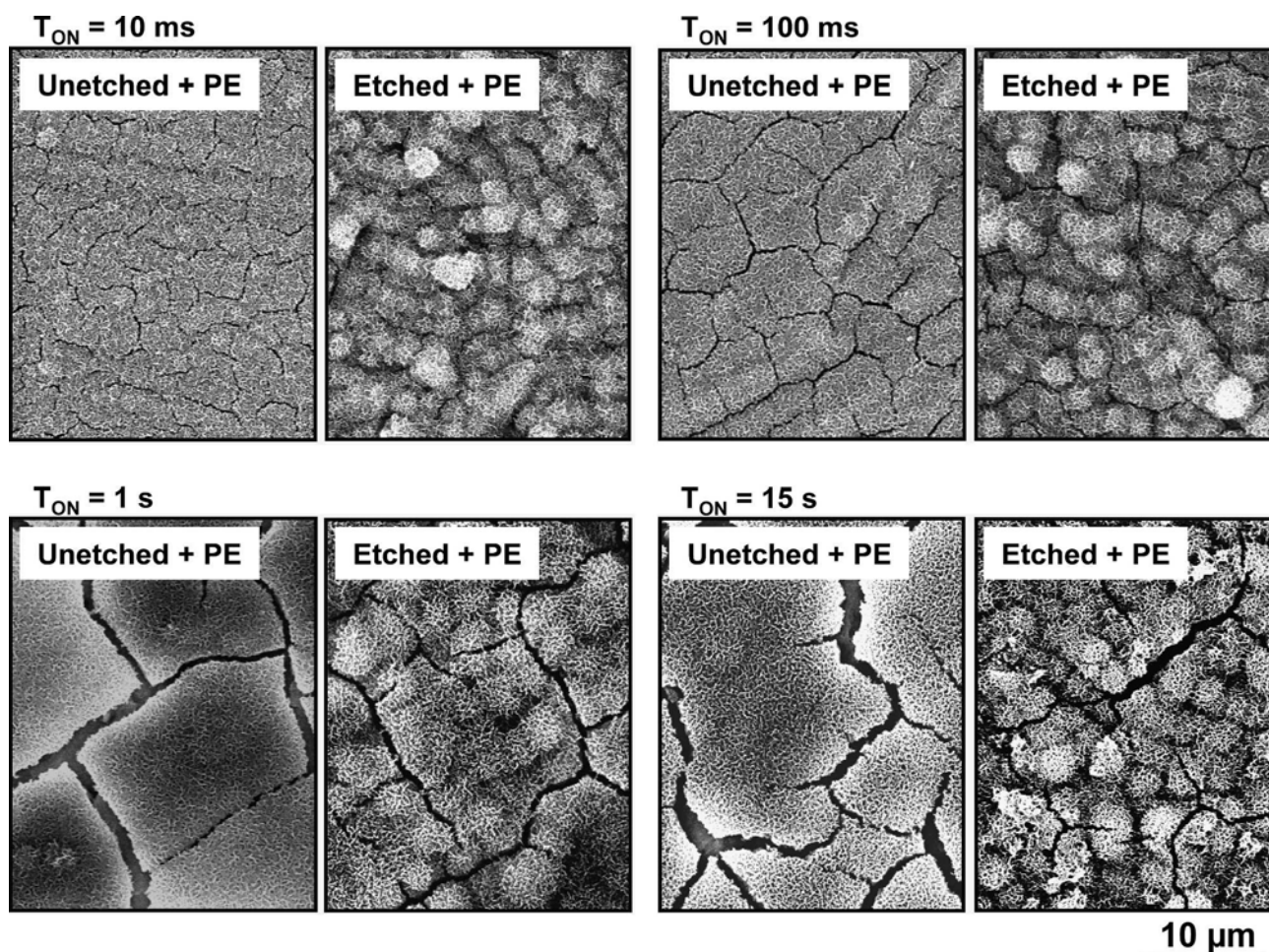


FIG. 7. FE-SEM photographs of unetched and etched Ti substrates subjected to electrodeposition at various  $T_{ON}$ .

the above peeling and scratch tests were summarized in Table II.

The mechanism for apatite formation and good adhesion on specimens electrodeposited under a short pulse

current at  $T_{ON}$  values, such as 10 ms, can be interpreted as follows. When the potential is loaded at the cathode (Ti), cations ( $H^+$ ,  $Na^+$ ,  $K^+$ , and  $Ca^{2+}$ ) in the electrolyte move to the surface of the cathode within 10–30 ms, and

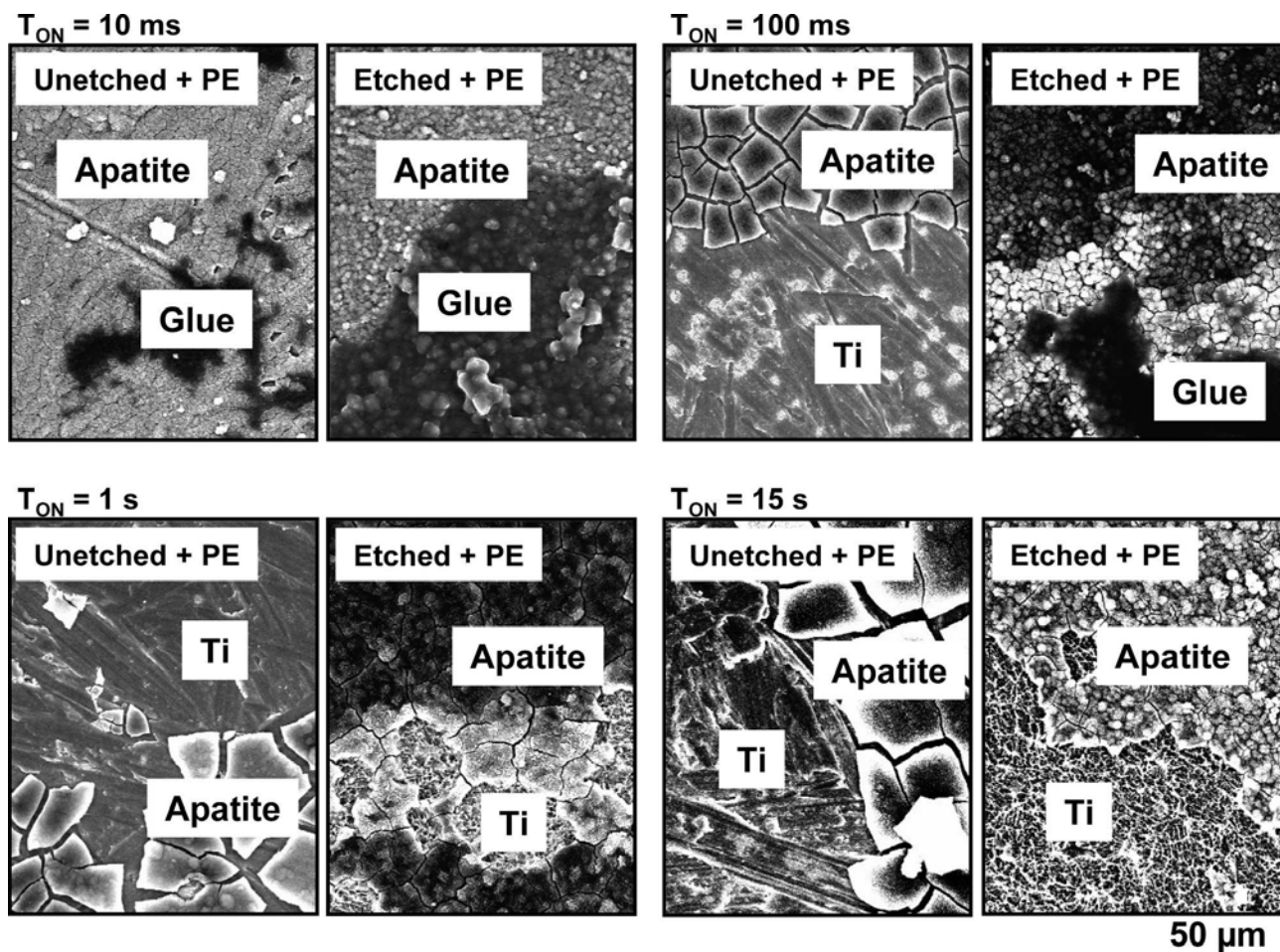
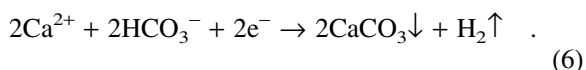
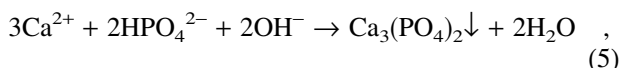
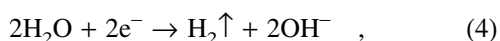


FIG. 8. FE-SEM photographs of unetched and etched Ti substrates subjected to electrodeposition at various  $T_{ON}$  followed by peeling test using Scotch tape.

then an electric double layer is formed.<sup>31</sup> In the electric double layer near the cathode, anions ( $\text{OH}^-$ ,  $\text{Cl}^-$ ,  $\text{HCO}_3^-$ , and  $\text{HPO}_4^-$ ) can exist due to diffusion. After the electric double layer is formed, the following reaction occurs at the surface of the cathode.<sup>17</sup>



Therefore, it is considered that the electric charge is consumed for the formation of the electric double layer and the reduction of  $\text{H}_2\text{O}$  during  $T_{ON}$ . Due to reaction (4), the pH value increases at the surface of the cathode. The sudden increase in pH triggers the crystal nucleation of C-P crystals.<sup>32</sup> The C-P crystals react with  $\text{H}_2\text{O}$  and  $\text{HCO}_3^-$  in the surrounding fluid to form apatite, including  $\text{CO}_3^{2-}$ . The decrease in  $T_{ON}$  causes an increase in the

TABLE II. Results for peeling and scratch tests.

$T_{ON}$	Unetched or etched	Peeling test	Scratch test
10 ms	Unetched	○	–
	Etched	○	○
100 ms	Unetched	X	–
	Etched	○	○
1 s	Unetched	X	–
	Etched	X	–
15 s	Unetched	X	–
	Etched	X	–

○, not peeled off or not coming off; X, peeled off; –, not measured.

consumption rate of the electric charge for the formation of the electric double layer per period. This means that both the reduction of  $\text{H}_2\text{O}$  and the amount of C-P crystal nuclei at the cathode surface per period decrease. As a result, it is considered that the nucleation of C-P crystals with low crystallinity occurred on the Ti surface without sufficiently reacting with other C-P crystals,  $\text{H}_2\text{O}$  and  $\text{HCO}_3^-$ , and hence small apatite crystals were deposited on the Ti surface. It is known that a residual stress in the

electrodeposited layer gives a large effect on their adhesive strength.<sup>33</sup> In this study, we speculate that the deposition of small apatite crystals increase the number of crystal grain boundary and hence decrease the residual stress that originated from the lattice mismatch between apatite crystals and Ti.<sup>33</sup> Therefore, the adhesive strength between apatite and the Ti substrates was enhanced for the specimen with  $T_{ON} = 10$  ms. As shown in Fig. 7, the adhesive strength was also enhanced at  $T_{ON} = 100$  ms for the etched Ti substrates subjected to PE. This can be attributed to the anchoring effect of the microstructural roughness formed during acid etching as well as the deposition of small apatite crystals. In conclusion, the electrodeposition technique described in this study is useful for coating bioactive apatite onto metallic materials.

#### IV. SUMMARY

Ti metal substrates etched in 75%  $H_2SO_4$  were roughened uniformly. Apatite films were deposited onto unetched substrates and substrates etched in 75%  $H_2SO_4$  by electrodeposition under a pulse current. For the specimens electrodeposited at  $T_{ON} = 10$  ms, the adhesive strength between apatite and the Ti substrates was greatly improved. In these specimens, we consider that the mismatch relaxation, which resulted from the difference in the lattice constant between apatite crystals and Ti, occurred due to the restraint of the growth of calcium phosphate into apatite.

#### ACKNOWLEDGMENT

This work was partially supported by Funds for Promoting Science and Technology under the Program for Exploring Advanced Interdisciplinary Frontiers, the Ministry of Education, Culture, Sports, Science and Technology, Japan.

#### REFERENCES

- H.B. Wen, J.R. de Wijn, F.Z. Cui, and K. de Groot: Preparation of bioactive  $Ti_6Al_4V$  surfaces by a simple method. *Biomaterials* **19**, 215 (1998).
- Y. Okazaki, E. Nishimura, E. Nakada, and K. Kobayashi: Surface analysis of Ti-15Zr-4Nb-4Ta alloy after implantation in rat tibia. *Biomaterials* **22**, 599 (2001).
- Y. Okazaki, S. Rao, Y. Ito, and T. Tateishi: Corrosion resistance, mechanical properties, corrosion fatigue strength and cytocompatibility of new Ti alloys without Al and V. *Biomaterials* **19**, 1197 (1998).
- U. Rolander, L. Mattsson, J. Lausmaa, and B. Kasemo: Anodic oxide films on titanium. *Ultramicroscopy* **19**, 407 (1986).
- H. Kienapfel, C. Sprey, A. Wilke, and P. Griss: Implant fixation by bone ingrowth. *J. Arthrop.* **14**, 355 (1999).
- T. Kitsugi, T. Nakamura, M. Oka, Y. Senaha, T. Goto, and T. Shibuya: Bone-bonding behavior of plasma-sprayed coatings of Bioglass®, AW-glass ceramic, and tricalcium phosphate on titanium alloy. *J. Biomed. Mater. Res.* **30**, 261 (1996).
- F. Barrere, C.A. Vanbitterswijk, K. Degroot, and P. Layrolle: Nucleation of biomimetic Ca-P coatings on  $Ti_6Al_4V$  from a SBF×5 solution: Influence of magnesium. *Biomaterials* **23**, 2211 (2002).
- T. Miyazaki, C. Ohtsuki, Y. Akioka, M. Tanihara, J. Nakao, Y. Sakaguchi, and S. Konagaya: Apatite deposition on polyamide films containing carboxyl group in a biomimetic solution. *J. Mater. Sci.-Mater. Med.* **14**, 569 (2003).
- S. Ban and J. Hasegawa: Morphological regulation and crystal growth of hydrothermal-electrochemically deposited apatite. *Biomaterials* **23**, 2965 (2002).
- A. Stoch, A. Brożek, G. Kmita, J. Stoch, W. Jastrzębski, and A. Rakowska: Electrophoretic coating of hydroxyapatite on titanium implants. *J. Mol. Struct.* **596**, 191 (2001).
- L.A. Sena, M.C. Andrade, A.M. Rossi, and G.A. Soares: Hydroxyapatite deposition by electrophoresis on titanium sheets with different surface finishing. *J. Biomed. Mater. Res. A* **60**, 1 (2002).
- Y. Fu, A.W. Batchelor, Y. Wang, and K.A. Khor: Fretting wear behaviors of thermal sprayed hydroxyapatite (HA) coating under unlubricated conditions. *Wear* **217**, 132 (1998).
- Y. Fu, A.W. Batchelor, and K.A. Khor: Fretting wear behavior of thermal sprayed hydroxyapatite coating lubricated with bovine albumin. *Wear* **230**, 98 (1999).
- H.C. Gledhill, I.G. Turner, and C. Doyle: In vitro fatigue behaviour of vacuum plasma and detonation gun sprayed hydroxyapatite coatings. *Biomaterials* **22**, 1233 (2001).
- M. Manso, C. Jimenez, C. Morant, P. Herrero, and J.M. Martinez-Duart: Electrodeposition of hydroxyapatite coatings in basic conditions. *Biomaterials* **21**, 1775 (2000).
- M. Kawashita, S. Itoh, K. Miyamoto, and G.H. Takaoka: Apatite formation on titanium substrates by electrochemical deposition in metastable calcium phosphate solution. *J. Mater. Sci.-Mater. Med.* **19**, 137 (2008).
- S. Ban: Development of electrochemical apatite-coating on titanium for biological application. *Phos. Res. Bull.* **17**, 9 (2004).
- S. Ban and S. Maruno: Effect of pH buffer on electrochemical deposition of calcium phosphate. *Jpn. J. Appl. Phys.* **32**, 1577 (1993).
- M. Kawashita, T. Hayakawa, and G.H. Takaoka: Electrochemical deposition of apatite on titanium substrates by using pulse current. *Key Eng. Mater.* **361-363**, 629 (2008).
- T. Hayakawa, M. Kawashita, and G.H. Takaoka: Coating of hydroxyapatite films on titanium substrates by electrodeposition under pulse current. *J. Ceram. Soc. Jpn.* **116**, 68 (2008).
- D.T. Zero, G. Cavaretta Siegel, J. Fu, and H. Li: Effect of pyrophosphate on fluoride enhanced remineralization after an erosive challenge. *Caries Res.* **34**, 344 (2000).
- T. Kokubo, H. Kushitani, S. Sakka, T. Kitsugi, and T. Yamamuro: Solutions able to reproduce in vivo surface-structure changes in bioactive glass-ceramic A-W. *J. Biomed. Mater. Res.* **24**, 721 (1990).
- N.C. Blumenthal: Mechanisms of inhibition of calcification. *Clin. Orthop. Relat. Res.* **247**, 279 (1989).
- S. Ban, Y. Iwaya, H. Kono, and H. Sato: Surface modification of titanium by etching in concentrated sulfuric acid. *Dent. Mater.* **22**, 1115 (2006).
- S. Ban and S. Maruno: Morphology and microstructure of electrochemically deposited calcium phosphates in a modified simulated body fluid. *Biomaterials* **19**, 1245 (1998).
- H.P. Klug and L.E. Alexander: *X-ray Diffraction Procedures*, 2nd ed. (Wiley & Sons Inc., New York, 1974), pp. 505, 565.
- H. Monma: Electrolytic depositions of calcium phosphates on substrate. *J. Mater. Sci.* **29**, 949 (1994).

28. C. Rey, B. Collins, T. Goehl, I.R. Dickson, and M.J. Glimcher: The carbonate environment in bone mineral: A resolution-enhanced Fourier transform infrared spectroscopy study. *Calcif. Tissue Int.* **45**, 157 (1989).
29. B.O. Fowler, E.C. Moneno, and W.E. Brown: Infra-red spectra of hydroxyapatite, octacalcium phosphate and pyrolysed octacalcium phosphate. *Arch. Oral Biol.* **11**, 477 (1966).
30. Y. Nonaka and Y. Morimoto: Characteristic and applications of amorphous chromium plating. *J. Surface Finish. Soc. Jpn.* **56**, 329 (2005).
31. J. Yamazaki, T. Kuranaga, H. Takaba, N. Saito, Y. Inoue, and O. Takai: Electrochromic response of obliquely sputtered InN films. *J. Surface Finish. Soc. Jpn.* **57**, 459 (2006).
32. S. Lin, R.Z. LeGeros, and J.P. LeGeros: Adherent octacalciumphosphate coating on titanium alloy using modulated electrochemical deposition method. *J. Biomed. Mater. Res. A* **66**, 819 (2003).
33. S. Haruyama: *Electrochemistry for Surface Engineers*, 2nd ed. (Maruzen, Tokyo, 2005), p. 171, in Japanese.